05,07

Microstructure, dielectric and ferroelectric characteristics of $0.1BiFeO_3-0.9PbFe_{0.5}Nb_{0.5}O_3$ multiferroic ceramics at temperatures of 10–850 K

© A.V. Pavlenko[1,2], K.M. Zhidel[1]

[1] Scientific Research Institute of Physics, Southern Federal University, Rostov-on-Don, Russia
[2] Scientific Research Institute of Physics, Southern Federal University, Rostov-on-Don, Russia

E-mail: karinagidele@gmail.com

Received December 25, 2024
Revised March 27, 2025
Accepted March 28, 2025

The microstructure, dielectric, ferroelectric and piezoelectric characteristics of the multiferroic ceramics $0.1BiFeO_3-0.9PbFe_{0.5}Nb_{0.5}O_3$ have been studied. It is shown that ceramics are impurity-free and have a homogeneous grain structure. When analyzing the $\varepsilon'(T, f)$ and $\varepsilon''(T, f)$ dependences of the sample at $T = (10-850)$ K, it was found that $0.1BiFeO_3-0.9PbFe_{0.5}Nb_{0.5}O_3$ is a relaxor ferroelectric; a magnetodielectric effect appears during the magnetic phase transition, and at $T > 450$ K, a significant contribution to the dielectric response begins to be made by the Maxwell–Wagner polarization and the corresponding dielectric relaxation. It was revealed that at room temperature, $0.1BiFeO_3-0.9PbFe_{0.5}Nb_{0.5}O_3$ ceramics, unlike $BiFeO_3$ and $PbFe_{0.5}Nb_{0.5}O_3$, is characterized by high values of the real part of the complex permittivity, $\varepsilon' \approx 9000$, dielectric controllability, $K \approx 40\,\%$ and a piezoelectric coefficient, $d_{33} \approx 340$ pm/V.

Keywords: solid solutions, dielectric controllability, ferroelectric relaxor, Maxwell–Wagner polarization.

DOI: 10.61011/PSS.2025.04.61270.352

1. Introduction

Nonlinear dielectric materials combining under certain conditions (temperature, pressure, etc.) ferroelectric (FE) and magnetic properties have attracted attention from both fundamental and applied perspectives in the last two decades [1]. This is not only attributable to their potential applications in functional electronics and sensorics due to the coupling between the ferroelectric and magnetic subsystems, but is also associated with the realization of new effects in them [2]. There are different approaches in creating such materials (synthesizing monocompounds, creating composites, etc.), but one of the most convenient and simple from the point of view of technology is to obtain solid solutions (SS) based on electrically and magnetically active compounds, such as lead ferroniobate ($PbFe_{0.5}Nb_{0.5}O_3$, PFN) and bismuth ferrite ($BiFeO_3$, BFO) [3].

PFN is a member of a family of multiferroics with a perovskite-type structure whose general chemical formula looks like $A(B'_{0.5}B''_{0.5})O_3$. A phase transition from the paraelectric (PE) to the FE phase takes place at the Curie temperature T_C, which is ~ 370 K [3,4]. The FE and antiferromagnetic (AFM) ordering coexist in PFN only below the Neel temperature T_N, in the range from 120 to 150 K [4]; however, despite this, the magnetodielectric effect (MDE) also occurs in it at $T > 300$ K [5,6]. BFO is also a multiferroic characterized by $T_C \approx 1103$ K and $T_N \approx 643$ K. Moreover, BFO is characterized by G-type antiferromagnetism with disproportionate cycloidal magnetic ordering in the [110] direction [3,7]. However, the high values of leakage currents and the great difficulty in obtaining impurity-free samples impose limitations on the study and use of BFO. The first phase diagram (PD) for the SS system of $(1-x)$BFO–xPFN [8] was developed in 1965. We have refined this diagram for room temperature in our paper in Ref. [9], defining the concentration intervals in which there are single-phase and morphotropic regions, as well as areas of coexistence of different phase states. Some studies observed that more promising characteristics are observed specifically in SS, in particular, the magnetoelectric effect is enhanced in SS with $x = 0.3$ and 0.4 according to [10] with the magnitude of the magnetoelectric coefficient α_{ME}reaching 2.5 mV/(cm · Oe) [11]. The literature analysis has shown that most attention in the SS system of $(1-x)$BFO–xPFN is paid to the compositions in the vicinity of the BFO; however, from our point of view, the compositions in the vicinity of the PFN may be of equal interest.

This paper describes the results of the study of the structure, dielectric and ferroelectric characteristics of ceramics with the composition 0.1BFO–0.9PFN located in the little-studied PD region of $(1-x)BiFeO_3-xPbFe_{0.5}Nb_{0.5}O_3$ — SS in the neighborhood of the morphotropic region of coexistence of pseudocubic and rhombohedral structures.

2. Research objects. Methods of fabrication and examination of samples

The SS with stoichiometric composition $0.1BiFeO_3-0.9PbFe_{0.5}Nb_{0.5}O_3$ was studied. The regulations for the synthesis of the material are provided in Ref. [9], the conformance of the elemental composition of the SS with the given stoichiometry was confirmed by X-ray fluorescence analysis [12]. A silver-containing paste was applied to the pre-polished surface of a ceramic disk with a diameter of 10 mm and thickness of 1 mm for dielectric and ferroelectric measurements. The grain structure of the samples was studied using Hitachi TM-1000 scanning electron microscope. Dielectric and mechanical hysteresis loops in the temperature range 293.15–363.15 K at frequency $f = 10$ Hz (signal shape is triangular) with external electric voltage values $U = 0 \pm 2$ kV were obtained using a measuring complex based on DX-FE2000 ferroelectric analyzer, thermal chamber, and a laser vibrometer. The values of residual and maximum polarizations (P_r and $P_{\max}$) and coercive field (E_c) of the studied samples were calculated using the analyzer software. The sample was placed in a specialized chamber cell filled with dielectric oil to perform measurements. The system was automatically calibrated immediately prior to the measurement.

Measurements of relative complex dielectric permittivity $\varepsilon^* = \varepsilon' - i\varepsilon''$ (ε' and ε'' — real and imaginary parts ε^* respectively) in the frequency range of $f = 200-2 \cdot 10^6$ Hz were performed using two automated measuring complexes. Measurements were performed at $T = (10-300)$ K using a bench based on WK 6500B precision impedance analyzer, and a bench based on an Agilent E4980A LCR meter and a Varta TP703 temperature controller was used for measurements at $T = (300-850)$ K.

The dielectric controllability K was calculated from experimental data obtained with a DX-FE2000 ferroelectric analyzer under stepwise variation of the external voltage $U = 0 \pm 1$ kV (step is 50 V, pulse duration is 10 s) at frequency $f = 10^3$ Hz and at room temperature, using the formula

$$K,\ \% = (\varepsilon'(0) - \varepsilon'(U))/\varepsilon'(0) \cdot 100, \qquad (1)$$

where $\varepsilon'(0)$ and $\varepsilon'(U)$ is the real part of the complex permittivity at $U = 0$ and at $U \neq 0$, respectively.

3. Experimental results and discussion

The formation of impurity-free 0.1BFO–0.9PFN ceramics, which had rhombohedral structure and relative density $\sim 90\,\%$ at room temperature, was found by X-ray diffraction analysis [9]. The electron microscopic results obtained by examining the prepared mechanical chip and the surface of the sintered ceramic block are presented in Figure 1 and testify in favor of the absence in the experimental sample of such impurity phases as Fe_2O_3, Bi_2O_3 and $Bi_2Fe_4O_9$, which

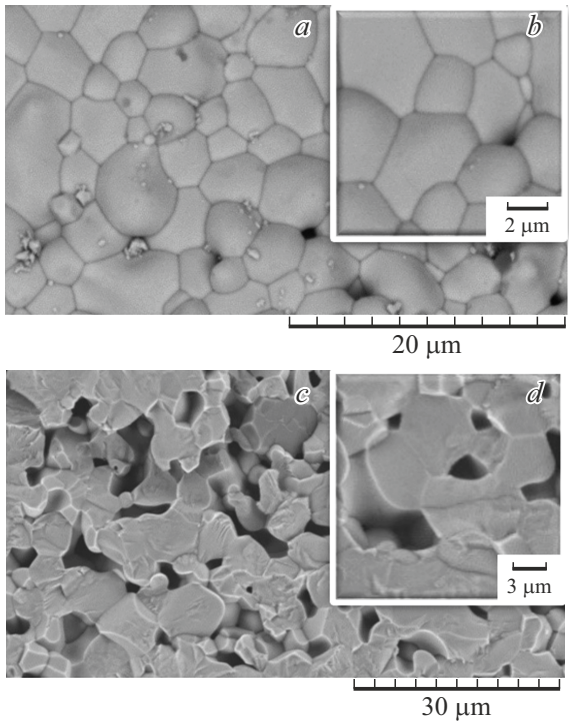

Figure 1. Fragment of the surface microstructure of sintered ceramic (a, b) and mechanical chip (c, d) of composition 0.1BFO–0.9PFN.

were previously found in BFO and PFN. The microstructure of 0.1BFO–0.9PFN ceramics is quite dense, homogeneous, and formed from irregular polygon-shaped crystallites with rounded boundaries and sizes ranging from 2 to 14 μm. The mechanical shear fracture occurred mainly along the grains themselves (Figure 1, $c-d$), which indicates the greater strength of the intergrain boundaries compared to the grain itself, in contrast to PFN and BFO, and suggests high internal homogeneity of the crystallites themselves.

Figures 2 and 3 show the dependences of $\varepsilon'(T, f)$ and $\varepsilon''(T, f)$ of 0.1BFO–0.9PFN ceramics in the temperature intervals of 10–300 and 300–850 K, respectively. A sharp increase of ε' is observed at all frequencies at $T = (10-300)$ K on the dependencies $\varepsilon'(T)$ of 0.1BFO–0.9PFN ceramics as the temperature increases from ~ 400 to ~ 9000 against the background of increasing dielectric dispersion $\Delta\varepsilon' = \big(\varepsilon'(f = 1\,\text{kHz}) - \varepsilon'(f = 1\,\text{MHz})\big)/\varepsilon'(f = 1\,\text{MHz})$. In the vicinity of 220 K (inset in Figure 2, b), an anomalous behavior is observed, manifested in the inflection points on the curve $\Delta\varepsilon'$ and the dependences $\varepsilon''(T)$, where the inflection points at high frequencies are transformed into maxima as f decreases. The phase transition from the paramagnetic (PM) phase to the AFM phase takes place in the vicinity of temperatures 210–220 K in SS 0.1BFO–0.9PFN according to the magnetic PD presented in Ref. [13]. Considering the latter, the revealed anomalous behavior of the dielectric parameters at $T = 220$ K is attributable to the MDE, which is manifested

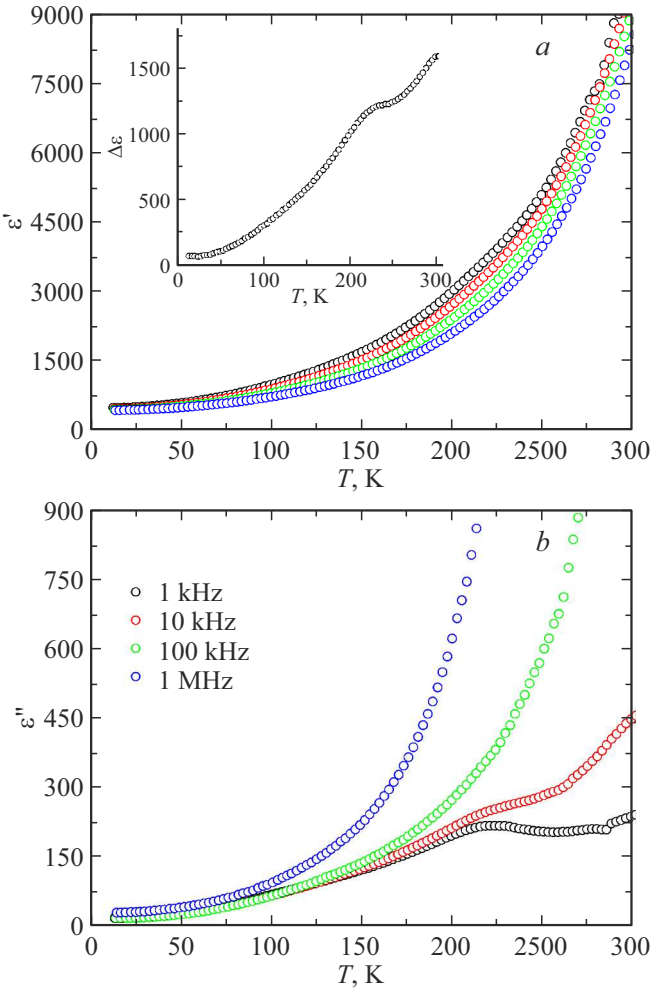

Figure 2. Dependences of $\varepsilon'(T, f)$ (a) and $\varepsilon''(T, f)$ (b) of 0.1BFO–0.9PFN ceramics in the temperature range of 10–300 K. Dielectric dispersion curve is shown in the inset $\Delta\varepsilon(T)$.

in multiferroics of this type in case of the magnetic phase transition [14]. It should be noted that unlike BFO and PFN, the values ε'' increase in 0.1BFO–0.9PFN ceramics at $T = (10–300)$ K with the increase of f, which is explained below.

A distinctive feature of the dependencies $\varepsilon'(T, f)$ of 0.1BFO–0.9PFN ceramics in the interval of $T = (300–850)$ K, unlike PFN and BFO, is the presence of two relaxing maxima at T_{m1} and T_{m2}, the temperature difference between which strongly depends on the measuring frequency. Relaxor ferroelectrics (RFE) are generally characterized by two maxima: $\varepsilon'(T, f)$ and $\varepsilon''(T, f)$. The first of these, $\varepsilon'(T, f)$, generally tends to decrease the height of the relaxation maximum with increasing frequency and temperature. The second maximum preceding the latter, $\varepsilon''(T, f)$, often exhibits the opposite trend, namely that the height of the relaxing maximum increases with increasing frequency and temperature. The maximum $\varepsilon'(T, f)$ at T_{m2} is characterized by a higher degree of blurring compared to T_{m1}, while its corresponding maximum $\varepsilon''(T, f)$ becomes indistinguishable at high frequencies. This is attributable to the increase in the through conductivity of the ceramics in this temperature range, which leads to the appearance of „humps“ in the dielectric response. The fact that ε' rapidly increases starting from temperatures being the higher the higher f at $T > T_{m2}$ after a sharp decline, and this is accompanied by a dispersion that increases as T increases. This is often observed in ceramic materials after the transition from the SE to PE phase, and is attributable to the following. While the material is in the FE phase and is broken into domains, the charges present in it due to defectivity are involved in polarization shielding and can be fixed on traps and domain walls. The spontaneous polarization disappears in case of the transition to the PE phase, the domain structure collapses and, as a consequence, the corresponding energy barriers disappear, which leads to an increase in the electrical conductivity of the material.

We observed two frequency-separated arcs of semicircles in the Cole–Cole diagrams (Figure 3, c–j) already at room temperature (the boundary f increases with increasing T), only one arc is observed at $T > 450$ K. These results indicate the occurrence of two relaxation processes in 0.1BFO–0.9PFN ceramics at $T = (10–850)$ K, which give the main contribution to the recorded dielectric response and prevail in different temperature ranges.

The former prevails at $T < 400$ K and is attributable to the occurrence of FE polarization in the studied material, while the latter prevails at $T > 400$ K and is attributable to the real (defective) structure of the material. It can be stated taking into account the results provided in Refs. [13,15] that the changes of ε' and ε'' at $T = (10–400)$ K are attributable to the phase transition RFE → PE. This is supported by the analysis of the dependence $T_{m1}(f)$ — the best results are achieved in the case of using the Vogel-Fulcher relation in case of approximation (Figure 4):

$$f = f_0 \exp\left(E_{act}/(k_B(T_m - T_{VF}))\right), \qquad (2)$$

where f_0 is the frequency of attempts to overcome the potential barrier E_{act}, k_B — Boltzmann constant, T_{VF} — Vogel-Fulcher temperature. Calculated values $E_{act} = 0.004$ eV, $f_0 = 8 \cdot 10^7$ Hz and $T_{VF} = 310$ K characteristic of RFE.

The value of the Burns temperature (T_B — the temperature at which polar regions appear in the RFE), estimated from the dependence of $(\varepsilon')^{-1}$ (T, $f = 1$ MHz), was $T_B \approx 450$ K (Figure 5). Although a comparison of the dependence $\varepsilon'(T, f)$ for PFN ceramics and 0.1BFO–0.9PFN ceramics shows a shift of the maxima to lower temperatures, the directly polar regions in our sample occur at higher temperatures. Occurrence of relaxor properties in 0.1BFO–0.9PFN ceramics is attributable to both the disordering of their structure (along A- and B-positions) and the specificity of the defective subsystem inherited from lead ferroniobate and bismuth ferrite [2,16].

X-ray diffraction studies of the ceramics showed no evidence of structure ordering at B-positions. It is known

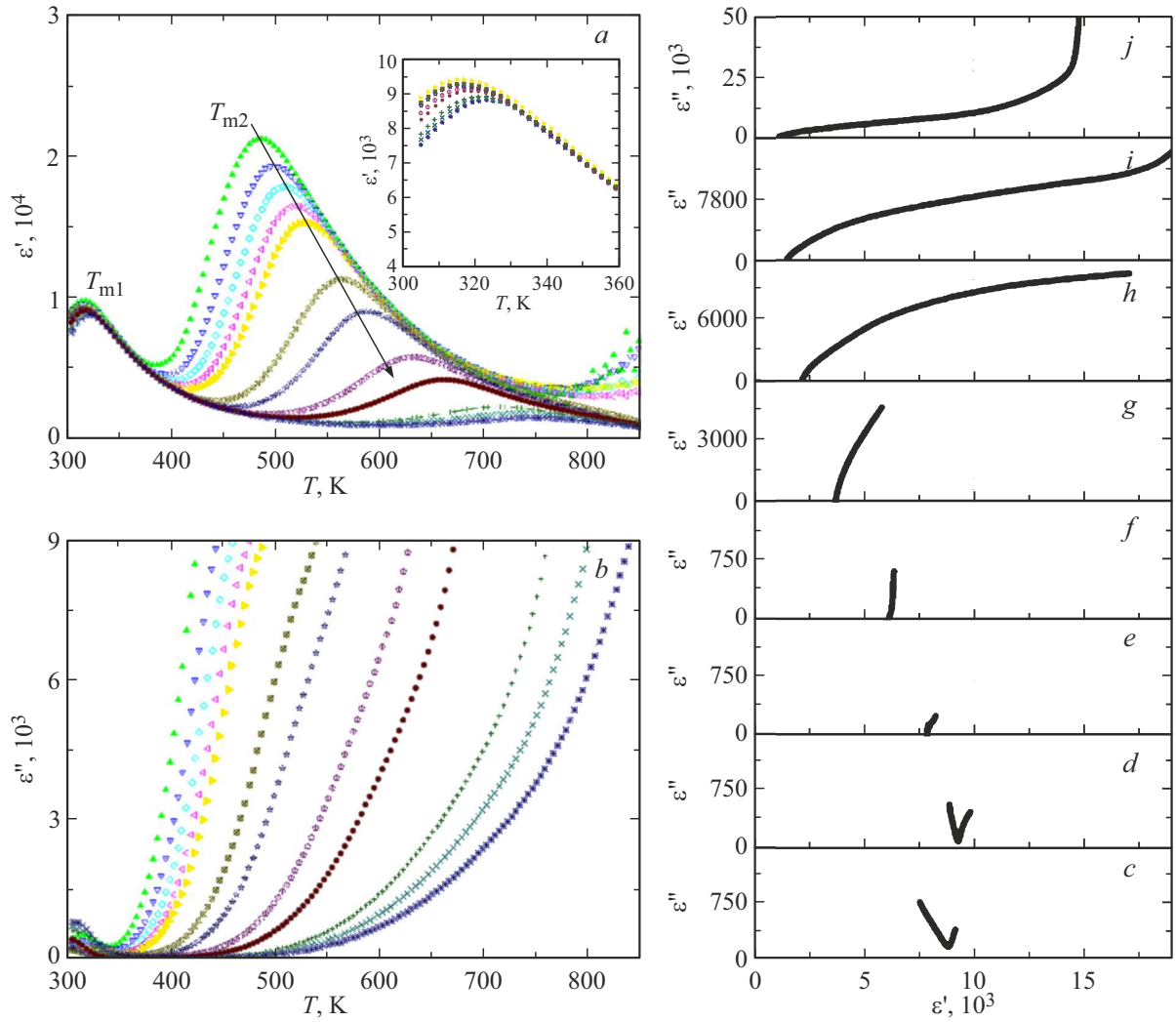

Figure 3. Dependences $\varepsilon'(T, f)$ (*a*) and $\varepsilon''(T, f)$ (*b*) of 0.1BFO–0.9PFN in the temperature range of 310–800 K and frequency range of 300–10^6 Hz. Cole–Cole diagrams for temperatures *c* — 300, *d* — 400, *e* — 450, *f* — 475, *g* — 500, *h* — 525, *i* — 550 and *j* — 600 K.

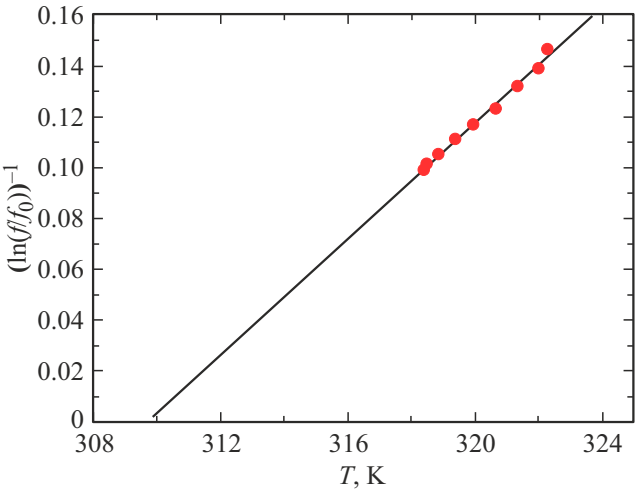

Figure 4. Illustration of the fulfillment of the Vogel-Fulcher relation in ceramics 0.1BFO–0.9PFN.

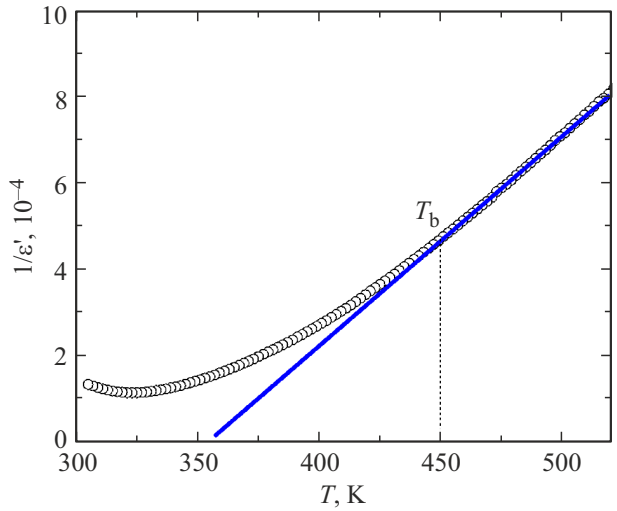

Figure 5. Dependence $(\varepsilon')^{-1}$ $(T, f = 1\,\text{MHz})$ for 0.1BFO–0.9PFN ceramics in the temperature range of 300–580 K. The solid line is-an illustration of the fulfillment of the Curie-Weiss law.

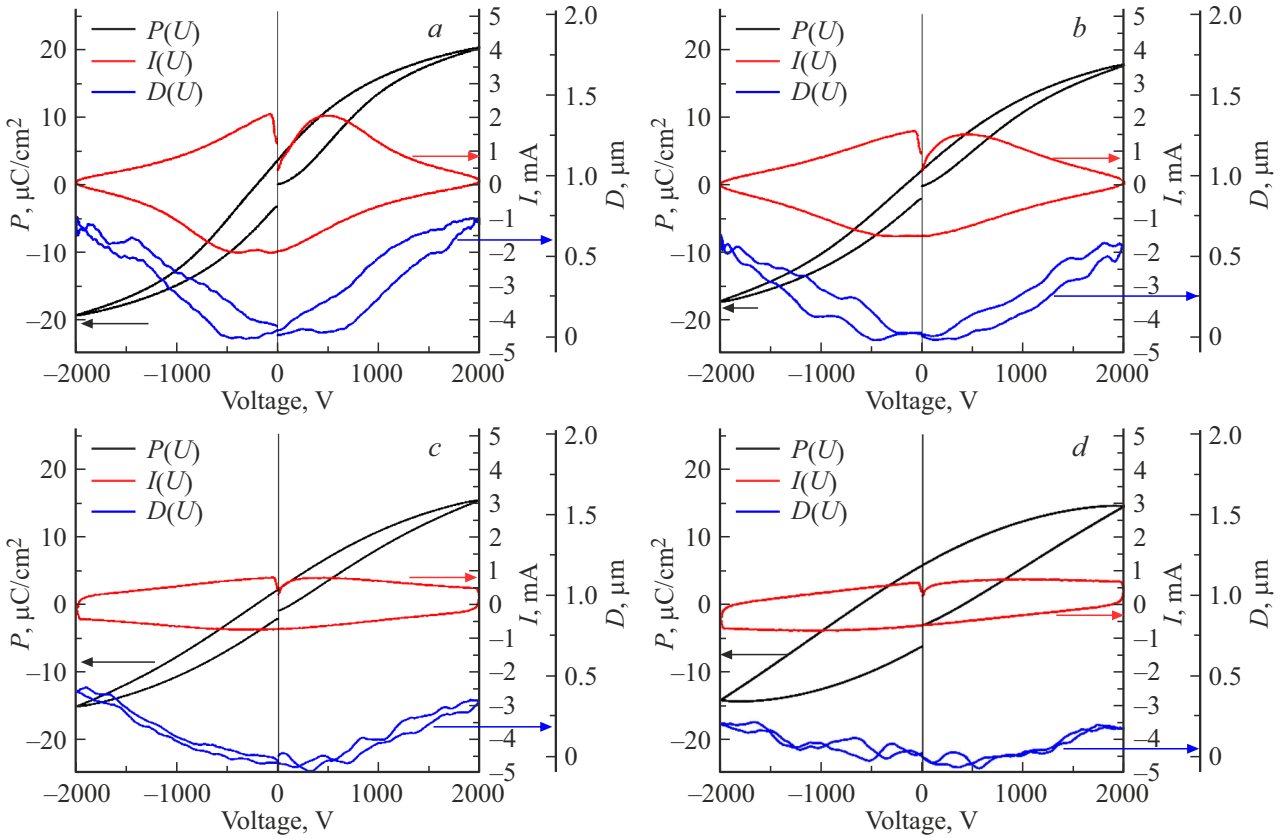

Figure 6. Dependences $P(U)$, $I(U)$ and $D(U)$ of SS ceramics of 0.1BFO–0.9PFN composition for temperatures *a* — 298, *b* — 313, *c* — 333, *d* — 353 K.

that no ordering of cations of type 1:1 takes place in lead ferroniobate in *B*-position [17], but the presence of Fe or Nb-rich regions is recorded [18]. In our case, the situation is further complicated and leads, as will be shown below, to the manifestation of a promising set of properties. Anomalous behavior of ε' and ε'' in 0.1BFO–0.9PFN ceramics at $T > 400$ K is essentially inherited from the PFN ceramics [4] and is attributable to the manifestation of the effects of Maxwell–Wagner (interlayer) polarization and its corresponding dielectric relaxation. Calculations have shown that a good agreement between the experimental and theoretical dependences $\varepsilon'(f)$ and $\varepsilon''(f)$ in this temperature range can be achieved using the dielectric model with the Cole-Cole relaxation time distribution function (i. e., the relaxation of the non-Debye type), while the dependence $T_{m2}(f)$ is described by the classical Arrhenius relation.

The dependences $P(U)$, $I(U)$ and $D(U)$ of 0.1BFO–0.9PFN ceramics at different temperatures are shown in Figure 6. Unlike PFN [4], the $P(U)$ loops in 0.1BFO–0.9PFN have an elongated shape with small hysteresis: $P_r = 3.16\,\mu$C/cm^2, $P_{\max} = 20.1\,\mu$C/cm^2, $E_c = 1.96$ kV/cm. The presence of hysteresis was also reflected in the material strain relationships $D(U)$, which had the shape of a „butterfly“, and the magnitude of the piezoelectric coefficient reached high values — $d_{33} \approx 340$ pm/V. The loops $P(U)$, $I(U)$, and $D(U)$ narrow

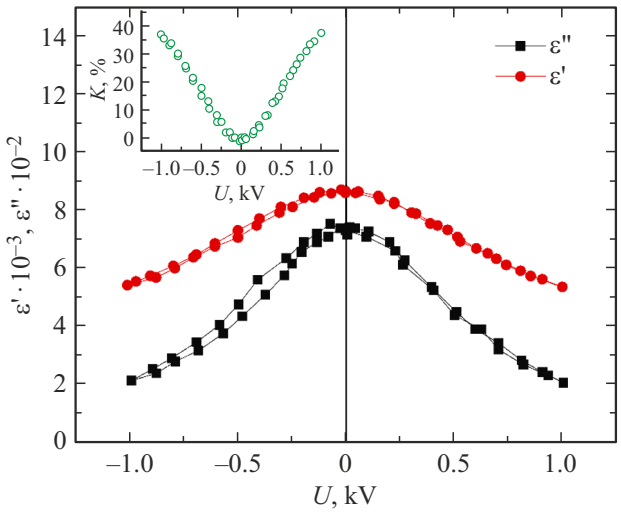

Figure 7. Dependences $\varepsilon'(U)$ and $\varepsilon''(U)$ of SS ceramics of composition 0.1BFO–0.9PFN at room temperature at $f = 100$ kHz. The dependence of the dielectric controllability $K(U)$ on the external electric field strength is shown on the inset.

with the temperature increase in case of the transition to the PE state, as expected, the values P_r, E_c and $P_{\max}$ decrease, and the loops $P(U)$ expand at temperatures above

370 K and round due to the increase in the conductivity of the ceramics. All these confirm that the phase transition RFE → PE takes place in the indicated temperature range.

As follows from Figure 7, the almost hysteresis-free variation of $\varepsilon'(U)$ and $\varepsilon''(U)$ is characteristic of 0.1BFO−0.9PFN ceramics, and both characteristics have a symmetric dome-shape with maxima at 0 V when an external electric field is applied. This confirms the small magnitudes of the coercive fields in the material.

The magnitude of dielectric controllability at an external electric field strength equal to 1 kV/mm reaches 40 % and is independent of the polarity of the applied voltage. This is attributable to the proximity to room temperature of the RFE → region of the PE phase transition, as well as the high values of ε', low values of ε'' and practically hysteresis-free character of their changes in the external electric field. All this indicates the promising use of this material in capacitors with variable capacitance.

4. Findings and conclusion

The microstructure analysis of 0.1BFO−0.9PFN ceramics found that it is quite dense, and the crystallites, which range in size from 2 to 14 μm, are in the form of irregular polyhedrons with predominantly rounded boundaries. No impurity phases were detected in the sample. The complex analysis of dielectric, ferroelectric and piezoelectric characteristics of the fabricated samples showed that the introduction of 10 % $BiFeO_3$ into lead ferroniobate results, on the one hand, in significant changes of the characteristics: the material becomes RFE, the value of dielectric permittivity ε' increases, dielectric controllability K and piezoelectric coefficient d_{33} increases, and on the other hand, the patterns of change of dependences $\varepsilon'/\varepsilon_0(T, f)$ and $\varepsilon''/\varepsilon_0(T, f)$, related to the specificity of the real structure, are preserved in the PE phase. Occurrence of the relaxor properties of 0.1BFO−0.9PFN and the increase of the Neel temperature (MDE-related anomalies were recorded in its vicinity on the dependences) $\varepsilon'/\varepsilon_0(T, f)$ and $\varepsilon''/\varepsilon_0(T, f)$ suggests that the crystallochemical disordering increases both in A-sublattice and in B-sublattice compared to PFN. The presented results can be used for the development of functional multiferroic materials based on the SS system $(1-x)BiFeO_3-xPbFe_{0.5}Nb_{0.5}O_3$.

Funding

The study was supported by the Ministry of Science and Higher Education of the Russian Federation (State assignment in the field of research. Project No. FENW-2023-0010/GZ0110/23-11-IF).

Acknowledgments

Equipment provided by the „Joint Scientific and Technological Equipment Center of the Southern Scientific Center of the Russian Academy of Sciences (Research, Development, Testing)“ shared research facility was used in the study.

Conflict of interest

The authors declare no conflict of interest.

References

[1] N.A. Spaldin, R. Ramesh. Nat. Mater. **18**, *3*, 203 (2019).
[2] N. Spaldin. Proc. Math. Phys. Eng. Sci. **476**, *2233*, 20190542 (2020).
[3] Yu.N. Venevtsev, V.V. Gagulin, V.N. Lyubimov. Segnetomagnetiki. Nauka, M. (1982). p. 224. (in Russian).
[4] A.V. Pavlenko, A.T. Kozakov, S.P. Kubrin, A.A. Pavelko, K.A. Guglev, L.A. Shilkina, I.A. Verbenko, D.A. Sarichev, L.A. Reznichenko. Ceram. Int. **38**, *8*, 6157 (2012).
[5] A.V. Turik, A.V. Pavlenko, K.P. Andryushin, S.I. Shevtsova, L.A. Reznichenko, A.I. Chernobabov. Phys. Solid State **54**, *5*, 947 (2012).
[6] O. Raymond, R. Font, J. Portelles, J.M. Siqueiros. J. Appl. Phys. **109**, *9*, 094106 (2011).
[7] A.M. Kadomtseva, Y.F. Popov, A.P. Pyatakov, G.P. Vorob'ev, A.K. Zvezdin, D. Viehland. Phase Transit. **79**, *12*, 1019 (2006).
[8] N.N. Krainik, N.P. Khuchua, A.A. Berezhnoy, A.G. Tutov. FTT **7**, *1*, 132 (1965).
[9] L.A. Shilkina, A.V. Pavlenko, L.A. Reznichenko, I.A. Verbenko. Crystallogr. Reps **61**, *2*, 263 (2016).
[10] J.P. Patel, A. Singh, D. Pandey. J. Appl. Phys. **107**, *10*, 104115 (2010).
[11] D. Bochenek, P. Niemiec, P. Guzdek, M. Wzorek. Mater. Chem. Phys. **195**, 199 (2017).
[12] A.S. Golofastova, N.M. Novikovsky, V.M. Raznomazov, A.V. Pavlenko, I.A. Verbeno, D.A. Sarychev, L.A. Reznichenko, A.V. Makhiboroda. UPF **4**, *1*, 32 (2016). (in Russian).
[13] E.G. Fesenko. Segnetoelectriki. Izd-vo Rostovskogo universiteta, Rostov-na-Donu (1968). p. 274. (in Russian).
[14] S. Dong, J.-M. Liu, S.-W. Cheong, Z. Ren. Adv. Phys. **64**, *5–6*, 519 (2015).
[15] V.V. Zhdanova. FTT **7**, *1*, 143 (1965).
[16] A.V. Pavlenko, L.A. Shilkina, L.A. Reznichenko. Crystallogr. Reps **57**, *1*, 118 (2012).
[17] V.P. Sakhnenko, N.V. Ter-Oganessian. Acta Crystallografica B. Struct. Sci. Cryst. Eng. Mater. **74**, *Part 3*, 264 (2018).
[18] Y. Yang, S.T. Zhang, H.B. Huang, Y.F. Chen, Z.G. Liu, J.-M. Liu. Mater. Lett. **59**, *14–15*, 1767 (2005).

Translated by A.Akhtyamov